

Measurement of the WW production cross section in $p\bar{p}$ collisions at $\sqrt{s} = 1.96$ TeV

V.M. Abazov,³³ B. Abbott,⁷⁰ M. Abolins,⁶¹ B.S. Acharya,²⁷ M. Adams,⁴⁸ T. Adams,⁴⁶ M. Agelou,¹⁷ J.-L. Agram,¹⁸ S.H. Ahn,²⁹ M. Ahsan,⁵⁵ G.D. Alexeev,³³ G. Alkhazov,³⁷ A. Alton,⁶⁰ G. Alverson,⁵⁹ G.A. Alves,² M. Anastasoae,³² S. Anderson,⁴² B. Andrieu,¹⁶ Y. Arnaud,¹³ A. Askew,⁷⁴ B. Åsman,³⁸ O. Atramentov,⁵³ C. Autermann,²⁰ C. Avila,⁷ F. Badaud,¹² A. Baden,⁵⁷ B. Baldin,⁴⁷ P.W. Balm,³¹ S. Banerjee,²⁷ E. Barberis,⁵⁹ P. Bargassa,⁷⁴ P. Baringer,⁵⁴ C. Barnes,⁴⁰ J. Barreto,² J.F. Bartlett,⁴⁷ U. Bassler,¹⁶ D. Bauer,⁵¹ A. Bean,⁵⁴ S. Beauceron,¹⁶ M. Begel,⁶⁶ A. Bellavance,⁶³ S.B. Beri,²⁶ G. Bernardi,¹⁶ R. Bernhard,^{47,*} I. Bertram,³⁹ M. Besançon,¹⁷ R. Beuselinck,⁴⁰ V.A. Bezzubov,³⁶ P.C. Bhat,⁴⁷ V. Bhatnagar,²⁶ M. Binder,²⁴ K.M. Black,⁵⁸ I. Blackler,⁴⁰ G. Blazey,⁴⁹ F. Blekman,³¹ S. Blessing,⁴⁶ D. Bloch,¹⁸ U. Blumenschein,²² A. Boehnlein,⁴⁷ O. Boeriu,⁵² T.A. Bolton,⁵⁵ F. Borchering,⁴⁷ G. Borisssov,³⁹ K. Bos,³¹ T. Bose,⁶⁵ A. Brandt,⁷² R. Brock,⁶¹ G. Brooijmans,⁶⁵ A. Bross,⁴⁷ N.J. Buchanan,⁴⁶ D. Buchholz,⁵⁰ M. Buehler,⁴⁸ V. Buescher,²² S. Burdin,⁴⁷ T.H. Burnett,⁷⁶ E. Busato,¹⁶ J.M. Butler,⁵⁸ J. Bystricky,¹⁷ W. Carvalho,³ B.C.K. Casey,⁷¹ N.M. Cason,⁵² H. Castilla-Valdez,³⁰ S. Chakrabarti,²⁷ D. Chakraborty,⁴⁹ K.M. Chan,⁶⁶ A. Chandra,²⁷ D. Chapin,⁷¹ F. Charles,¹⁸ E. Cheu,⁴² L. Chevalier,¹⁷ D.K. Cho,⁶⁶ S. Choi,⁴⁵ T. Christiansen,²⁴ L. Christofek,⁵⁴ D. Claes,⁶³ B. Clément,¹⁸ C. Clément,³⁸ Y. Coadou,⁵ M. Cooke,⁷⁴ W.E. Cooper,⁴⁷ D. Coppage,⁵⁴ M. Corcoran,⁷⁴ J. Coss,¹⁹ A. Cothenet,¹⁴ M.-C. Cousinou,¹⁴ S. Crépe-Renaudin,¹³ M. Cristetiu,⁴⁵ M.A.C. Cummings,⁴⁹ D. Cutts,⁷¹ H. da Motta,² B. Davies,³⁹ G. Davies,⁴⁰ G.A. Davis,⁵⁰ K. De,⁷² P. de Jong,³¹ S.J. de Jong,³² E. De La Cruz-Burelo,³⁰ C. De Oliveira Martins,³ S. Dean,⁴¹ F. Déliot,¹⁷ P.A. Delsart,¹⁹ M. Demarteau,⁴⁷ R. Demina,⁶⁶ P. Demine,¹⁷ D. Denisov,⁴⁷ S.P. Denisov,³⁶ S. Desai,⁶⁷ H.T. Diehl,⁴⁷ M. Diesburg,⁴⁷ M. Doidge,³⁹ H. Dong,⁶⁷ S. Doulas,⁵⁹ L. Duflot,¹⁵ S.R. Dugad,²⁷ A. Duperrin,¹⁴ J. Dyer,⁶¹ A. Dyshkant,⁴⁹ M. Eads,⁴⁹ D. Edmunds,⁶¹ T. Edwards,⁴¹ J. Ellison,⁴⁵ J. Elmsheuser,²⁴ J.T. Eltzroth,⁷² V.D. Elvira,⁴⁷ S. Eno,⁵⁷ P. Ermolov,³⁵ O.V. Eroshin,³⁶ J. Estrada,⁴⁷ D. Evans,⁴⁰ H. Evans,⁶⁵ A. Evdokimov,³⁴ V.N. Evdokimov,³⁶ J. Fast,⁴⁷ S.N. Fatakia,⁵⁸ L. Felgioni,⁵⁸ T. Ferbel,⁶⁶ F. Fiedler,²⁴ F. Filthaut,³² W. Fisher,⁶⁴ H.E. Fisk,⁴⁷ M. Fortner,⁴⁹ H. Fox,²² W. Freeman,⁴⁷ S. Fu,⁴⁷ S. Fuess,⁴⁷ T. Gadfort,⁷⁶ C.F. Galea,³² E. Gallas,⁴⁷ E. Galyaev,⁵² C. Garcia,⁶⁶ A. Garcia-Bellido,⁷⁶ J. Gardner,⁵⁴ V. Gavrilov,³⁴ P. Gay,¹² D. Gelé,¹⁸ R. Gelhaus,⁴⁵ K. Genser,⁴⁷ C.E. Gerber,⁴⁸ Y. Gershtein,⁷¹ G. Ginther,⁶⁶ T. Golling,²¹ B. Gómez,⁷ K. Gounder,⁴⁷ A. Goussiou,⁵² P.D. Grannis,⁶⁷ S. Greder,¹⁸ H. Greenlee,⁴⁷ Z.D. Greenwood,⁵⁶ E.M. Gregores,⁴ Ph. Gris,¹² J.-F. Grivaz,¹⁵ L. Groer,⁶⁵ S. Grünendahl,⁴⁷ M.W. Grunewald,²⁸ S.N. Gurzhiev,³⁶ G. Gutierrez,⁴⁷ P. Gutierrez,⁷⁰ A. Haas,⁶⁵ N.J. Hadley,⁵⁷ S. Hagopian,⁴⁶ I. Hall,⁷⁰ R.E. Hall,⁴⁴ C. Han,⁶⁰ L. Han,⁴¹ K. Hanagaki,⁴⁷ K. Harder,⁵⁵ R. Harrington,⁵⁹ J.M. Hauptman,⁵³ R. Hauser,⁶¹ J. Hays,⁵⁰ T. Hebbeker,²⁰ D. Hedin,⁴⁹ J.M. Heinmiller,⁴⁸ A.P. Heinson,⁴⁵ U. Heintz,⁵⁸ C. Hensel,⁵⁴ G. Hesketh,⁵⁹ M.D. Hildreth,⁵² R. Hirsosky,⁷⁵ J.D. Hobbs,⁶⁷ B. Hoeneisen,¹¹ M. Hohlfield,²³ S.J. Hong,²⁹ R. Hooper,⁷¹ P. Houben,³¹ Y. Hu,⁶⁷ J. Huang,⁵¹ I. Iashvili,⁴⁵ R. Illingworth,⁴⁷ A.S. Ito,⁴⁷ S. Jabeen,⁵⁴ M. Jaffré,¹⁵ S. Jain,⁷⁰ V. Jain,⁶⁸ K. Jakobs,²² A. Jenkins,⁴⁰ R. Jesik,⁴⁰ K. Johns,⁴² M. Johnson,⁴⁷ A. Jonckheere,⁴⁷ P. Jonsson,⁴⁰ H. Jöstlein,⁴⁷ A. Juste,⁴⁷ M.M. Kado,⁴³ D. Käfer,²⁰ W. Kahl,⁵⁵ S. Kahn,⁶⁸ E. Kajfasz,¹⁴ A.M. Kalinin,³³ J. Kalk,⁶¹ D. Karmanov,³⁵ J. Kasper,⁵⁸ D. Kau,⁴⁶ R. Kehoe,⁷³ S. Kermiche,¹⁴ S. Kesisoglou,⁷¹ A. Khanov,⁶⁶ A. Kharchilava,⁵² Y.M. Kharzheev,³³ K.H. Kim,²⁹ B. Klima,⁴⁷ M. Klute,²¹ J.M. Kohli,²⁶ M. Kopal,⁷⁰ V.M. Korablev,³⁶ J. Kotcher,⁶⁸ B. Kothari,⁶⁵ A. Koubarovsky,³⁵ A.V. Kozelov,³⁶ J. Kozminski,⁶¹ S. Krzywdzinski,⁴⁷ S. Kuleshov,³⁴ Y. Kulik,⁴⁷ S. Kunori,⁵⁷ A. Kupco,¹⁷ T. Kurča,¹⁹ S. Lager,³⁸ N. Lahrichi,¹⁷ G. Landsberg,⁷¹ J. Lazoflores,⁴⁶ A.-C. Le Bihan,¹⁸ P. Lebrun,¹⁹ S.W. Lee,²⁹ W.M. Lee,⁴⁶ A. Leflat,³⁵ F. Lehner,^{47,*} C. Leonidopoulos,⁶⁵ P. Lewis,⁴⁰ J. Li,⁷² Q.Z. Li,⁴⁷ J.G.R. Lima,⁴⁹ D. Lincoln,⁴⁷ S.L. Linn,⁴⁶ J. Linnemann,⁶¹ V.V. Lipaev,³⁶ R. Lipton,⁴⁷ L. Lobo,⁴⁰ A. Lobodenko,³⁷ M. Lokajicek,¹⁰ A. Lounis,¹⁸ H.J. Lubatti,⁷⁶ L. Lueking,⁴⁷ M. Lynker,⁵² A.L. Lyon,⁴⁷ A.K.A. Maciel,⁴⁹ R.J. Madaras,⁴³ P. Mättig,²⁵ A. Magerkurth,⁶⁰ A.-M. Magnan,¹³ N. Makovec,¹⁵ P.K. Mal,²⁷ S. Malik,⁵⁶ V.L. Malyshev,³³ H.S. Mao,⁶ Y. Maravin,⁴⁷ M. Martens,⁴⁷ S.E.K. Mattingly,⁷¹ A.A. Mayorov,³⁶ R. McCarthy,⁶⁷ R. McCroskey,⁴² D. Meder,²³ H.L. Melanson,⁴⁷ A. Melnitchouk,⁶² M. Merkin,³⁵ K.W. Merritt,⁴⁷ A. Meyer,²⁰ H. Miettinen,⁷⁴ D. Mihalcea,⁴⁹ J. Mitrevski,⁶⁵ N. Mokhov,⁴⁷ J. Molina,³ N.K. Mondal,²⁷ H.E. Montgomery,⁴⁷ R.W. Moore,⁵ G.S. Muanza,¹⁹ M. Mulders,⁴⁷ Y.D. Mutaf,⁶⁷ E. Nagy,¹⁴ M. Narain,⁵⁸ N.A. Naumann,³² H.A. Neal,⁶⁰ J.P. Negret,⁷ S. Nelson,⁴⁶ P. Neustroev,³⁷ C. Noeding,²² A. Nomerotski,⁴⁷ S.F. Novaes,⁴ T. Nunnemann,²⁴ E. Nurse,⁴¹ V. O'Dell,⁴⁷ D.C. O'Neil,⁵ V. Oguri,³ N. Oliveira,³ N. Oshima,⁴⁷ G.J. Otero y Garzón,⁴⁸ P. Padley,⁷⁴ N. Parashar,⁵⁶ J. Park,²⁹ S.K. Park,²⁹ J. Parsons,⁶⁵ R. Partridge,⁷¹ N. Parua,⁶⁷ A. Patwa,⁶⁸ P.M. Perea,⁴⁵ E. Perez,¹⁷ O. Peters,³¹

P. Pétrouff,¹⁵ M. Petteni,⁴⁰ L. Phaf,³¹ R. Piegai,¹ P.L.M. Podesta-Lerma,³⁰ V.M. Podstavkov,⁴⁷ Y. Pogorelov,⁵² B.G. Pope,⁶¹ W.L. Prado da Silva,³ H.B. Prosper,⁴⁶ S. Protopopescu,⁶⁸ M.B. Przybycien,^{50,†} J. Qian,⁶⁰ A. Quadt,²¹ B. Quinn,⁶² K.J. Rani,²⁷ P.A. Rapidis,⁴⁷ P.N. Ratoff,³⁹ N.W. Reay,⁵⁵ S. Reucroft,⁵⁹ M. Rijssenbeek,⁶⁷ I. Ripp-Baudot,¹⁸ F. Rizatdinova,⁵⁵ C. Royon,¹⁷ P. Rubinov,⁴⁷ R. Ruchti,⁵² G. Sajot,¹³ A. Sánchez-Hernández,³⁰ M.P. Sanders,⁴¹ A. Santoro,³ G. Savage,⁴⁷ L. Sawyer,⁵⁶ T. Scanlon,⁴⁰ R.D. Schamberger,⁶⁷ H. Schellman,⁵⁰ P. Schieferdecker,²⁴ C. Schmitt,²⁵ A.A. Schukin,³⁶ A. Schwartzman,⁶⁴ R. Schwienhorst,⁶¹ S. Sengupta,⁴⁶ H. Severini,⁷⁰ E. Shabalina,⁴⁸ M. Shamim,⁵⁵ V. Shary,¹⁷ W.D. Shephard,⁵² D. Shpakov,⁵⁹ R.A. Sidwell,⁵⁵ V. Simak,⁹ V. Sirotenko,⁴⁷ P. Skubic,⁷⁰ P. Slattery,⁶⁶ R.P. Smith,⁴⁷ K. Smolek,⁹ G.R. Snow,⁶³ J. Snow,⁶⁹ S. Snyder,⁶⁸ S. Söldner-Rembold,⁴¹ X. Song,⁴⁹ Y. Song,⁷² L. Sonnenschein,⁵⁸ A. Sopczak,³⁹ M. Sosebee,⁷² K. Soustruznik,⁸ M. Souza,² B. Spurlock,⁷² N.R. Stanton,⁵⁵ J. Stark,¹³ J. Steele,⁵⁶ G. Steinbrück,⁶⁵ K. Stevenson,⁵¹ V. Stolin,³⁴ A. Stone,⁴⁸ D.A. Stoyanova,³⁶ J. Strandberg,³⁸ M.A. Strang,⁷² M. Strauss,⁷⁰ R. Ströhmer,²⁴ M. Strovink,⁴³ L. Stutte,⁴⁷ S. Sumowidagdo,⁴⁶ A. Sznajder,³ M. Talby,¹⁴ P. Tamburello,⁴² W. Taylor,⁵ P. Telford,⁴¹ J. Temple,⁴² S. Tentindo-Repond,⁴⁶ E. Thomas,¹⁴ B. Thooris,¹⁷ M. Tomoto,⁴⁷ T. Toole,⁵⁷ J. Torborg,⁵² S. Towers,⁶⁷ T. Trefzger,²³ S. Trincaz-Duvoid,¹⁶ B. Tuchming,¹⁷ C. Tully,⁶⁴ A.S. Turcot,⁶⁸ P.M. Tuts,⁶⁵ L. Uvarov,³⁷ S. Uvarov,³⁷ S. Uzunyan,⁴⁹ B. Vachon,⁵ R. Van Kooten,⁵¹ W.M. van Leeuwen,³¹ N. Varelas,⁴⁸ E.W. Varnes,⁴² I.A. Vasilyev,³⁶ M. Vaupel,²⁵ P. Verdier,¹⁵ L.S. Vertogradov,³³ M. Verzocchi,⁵⁷ F. Villeneuve-Seguié,⁴⁰ J.-R. Vlimant,¹⁶ E. Von Toerne,⁵⁵ M. Vreeswijk,³¹ T. Vu Anh,¹⁵ H.D. Wahl,⁴⁶ R. Walker,⁴⁰ L. Wang,⁵⁷ Z.-M. Wang,⁶⁷ J. Warchol,⁵² M. Warsinsky,²¹ G. Watts,⁷⁶ M. Wayne,⁵² M. Weber,⁴⁷ H. Weerts,⁶¹ M. Wegner,²⁰ N. Wermes,²¹ A. White,⁷² V. White,⁴⁷ D. Whiteson,⁴³ D. Wicke,⁴⁷ D.A. Wijngaarden,³² G.W. Wilson,⁵⁴ S.J. Wimpenny,⁴⁵ J. Wittlin,⁵⁸ M. Wobisch,⁴⁷ J. Womersley,⁴⁷ D.R. Wood,⁵⁹ T.R. Wyatt,⁴¹ Q. Xu,⁶⁰ N. Xuan,⁵² R. Yamada,⁴⁷ M. Yan,⁵⁷ T. Yasuda,⁴⁷ Y.A. Yatsunenko,³³ Y. Yen,²⁵ K. Yip,⁶⁸ S.W. Youn,⁵⁰ J. Yu,⁷² A. Yurkewicz,⁶¹ A. Zabi,¹⁵ A. Zatserklyaniy,⁴⁹ M. Zdrzil,⁶⁷ C. Zeitnitz,²³ D. Zhang,⁴⁷ X. Zhang,⁷⁰ T. Zhao,⁷⁶ Z. Zhao,⁶⁰ B. Zhou,⁶⁰ J. Zhu,⁵⁷ M. Zielinski,⁶⁶ D. Zieminska,⁵¹ A. Zieminski,⁵¹ R. Zitoun,⁶⁷ V. Zutshi,⁴⁹ E.G. Zverev,³⁵ and A. Zylberstejn¹⁷
(DØ Collaboration)

¹ *Universidad de Buenos Aires, Buenos Aires, Argentina*

² *LAFEX, Centro Brasileiro de Pesquisas Físicas, Rio de Janeiro, Brazil*

³ *Universidade do Estado do Rio de Janeiro, Rio de Janeiro, Brazil*

⁴ *Instituto de Física Teórica, Universidade Estadual Paulista, São Paulo, Brazil*

⁵ *Simon Fraser University, Burnaby, Canada, University of Alberta, Edmonton, Canada, McGill University, Montreal, Canada and York University, Toronto, Canada*

⁶ *Institute of High Energy Physics, Beijing, People's Republic of China*

⁷ *Universidad de los Andes, Bogotá, Colombia*

⁸ *Charles University, Center for Particle Physics, Prague, Czech Republic*

⁹ *Czech Technical University, Prague, Czech Republic*

¹⁰ *Institute of Physics, Academy of Sciences, Center for Particle Physics, Prague, Czech Republic*

¹¹ *Universidad San Francisco de Quito, Quito, Ecuador*

¹² *Laboratoire de Physique Corpusculaire, IN2P3-CNRS, Université Blaise Pascal, Clermont-Ferrand, France*

¹³ *Laboratoire de Physique Subatomique et de Cosmologie, IN2P3-CNRS, Université de Grenoble 1, Grenoble, France*

¹⁴ *CPPM, IN2P3-CNRS, Université de la Méditerranée, Marseille, France*

¹⁵ *Laboratoire de l'Accélérateur Linéaire, IN2P3-CNRS, Orsay, France*

¹⁶ *LPNHE, Universités Paris VI and VII, IN2P3-CNRS, Paris, France*

¹⁷ *DAPNIA/Service de Physique des Particules, CEA, Saclay, France*

¹⁸ *IReS, IN2P3-CNRS, Université Louis Pasteur, Strasbourg, France and Université de Haute Alsace, Mulhouse, France*

¹⁹ *Institut de Physique Nucléaire de Lyon, IN2P3-CNRS, Université Claude Bernard, Villeurbanne, France*

²⁰ *RWTH Aachen, III. Physikalisches Institut A, Aachen, Germany*

²¹ *Universität Bonn, Physikalisches Institut, Bonn, Germany*

²² *Universität Freiburg, Physikalisches Institut, Freiburg, Germany*

²³ *Universität Mainz, Institut für Physik, Mainz, Germany*

²⁴ *Ludwig-Maximilians-Universität München, München, Germany*

²⁵ *Fachbereich Physik, University of Wuppertal, Wuppertal, Germany*

²⁶ *Panjab University, Chandigarh, India*

²⁷ *Tata Institute of Fundamental Research, Mumbai, India*

²⁸ *University College Dublin, Dublin, Ireland*

²⁹ *Korea Detector Laboratory, Korea University, Seoul, Korea*

³⁰ *CINVESTAV, Mexico City, Mexico*

³¹ *FOM-Institute NIKHEF and University of Amsterdam/NIKHEF, Amsterdam, The Netherlands*

³² *University of Nijmegen/NIKHEF, Nijmegen, The Netherlands*

³³ *Joint Institute for Nuclear Research, Dubna, Russia*

- ³⁴*Institute for Theoretical and Experimental Physics, Moscow, Russia*
³⁵*Moscow State University, Moscow, Russia*
³⁶*Institute for High Energy Physics, Protvino, Russia*
³⁷*Petersburg Nuclear Physics Institute, St. Petersburg, Russia*
³⁸*Lund University, Lund, Sweden, Royal Institute of Technology and Stockholm University, Stockholm, Sweden and Uppsala University, Uppsala, Sweden*
³⁹*Lancaster University, Lancaster, United Kingdom*
⁴⁰*Imperial College, London, United Kingdom*
⁴¹*University of Manchester, Manchester, United Kingdom*
⁴²*University of Arizona, Tucson, Arizona 85721, USA*
⁴³*Lawrence Berkeley National Laboratory and University of California, Berkeley, California 94720, USA*
⁴⁴*California State University, Fresno, California 93740, USA*
⁴⁵*University of California, Riverside, California 92521, USA*
⁴⁶*Florida State University, Tallahassee, Florida 32306, USA*
⁴⁷*Fermi National Accelerator Laboratory, Batavia, Illinois 60510, USA*
⁴⁸*University of Illinois at Chicago, Chicago, Illinois 60607, USA*
⁴⁹*Northern Illinois University, DeKalb, Illinois 60115, USA*
⁵⁰*Northwestern University, Evanston, Illinois 60208, USA*
⁵¹*Indiana University, Bloomington, Indiana 47405, USA*
⁵²*University of Notre Dame, Notre Dame, Indiana 46556, USA*
⁵³*Iowa State University, Ames, Iowa 50011, USA*
⁵⁴*University of Kansas, Lawrence, Kansas 66045, USA*
⁵⁵*Kansas State University, Manhattan, Kansas 66506, USA*
⁵⁶*Louisiana Tech University, Ruston, Louisiana 71272, USA*
⁵⁷*University of Maryland, College Park, Maryland 20742, USA*
⁵⁸*Boston University, Boston, Massachusetts 02215, USA*
⁵⁹*Northeastern University, Boston, Massachusetts 02115, USA*
⁶⁰*University of Michigan, Ann Arbor, Michigan 48109, USA*
⁶¹*Michigan State University, East Lansing, Michigan 48824, USA*
⁶²*University of Mississippi, University, Mississippi 38677, USA*
⁶³*University of Nebraska, Lincoln, Nebraska 68588, USA*
⁶⁴*Princeton University, Princeton, New Jersey 08544, USA*
⁶⁵*Columbia University, New York, New York 10027, USA*
⁶⁶*University of Rochester, Rochester, New York 14627, USA*
⁶⁷*State University of New York, Stony Brook, New York 11794, USA*
⁶⁸*Brookhaven National Laboratory, Upton, New York 11973, USA*
⁶⁹*Langston University, Langston, Oklahoma 73050, USA*
⁷⁰*University of Oklahoma, Norman, Oklahoma 73019, USA*
⁷¹*Brown University, Providence, Rhode Island 02912, USA*
⁷²*University of Texas, Arlington, Texas 76019, USA*
⁷³*Southern Methodist University, Dallas, Texas 75275, USA*
⁷⁴*Rice University, Houston, Texas 77005, USA*
⁷⁵*University of Virginia, Charlottesville, Virginia 22901, USA*
⁷⁶*University of Washington, Seattle, Washington 98195, USA*

(Dated: October 22, 2004)

We present a measurement of the W boson pair-production cross section in $p\bar{p}$ collisions at a center-of-mass energy of $\sqrt{s} = 1.96$ TeV. The data, collected with the Run II DØ detector, correspond to an integrated luminosity of 224–252 pb^{-1} depending on the final state (e^+e^- , $e^\pm\mu^\mp$ or $\mu^+\mu^-$). We observe 25 candidates with a background expectation of $8.1 \pm 0.6(\text{stat}) \pm 0.6(\text{syst}) \pm 0.5(\text{lum})$ events. The probability for an upward fluctuation of the background to produce the observed signal is 2.3×10^{-7} , equivalent to 5.2 standard deviations. The measurement yields a cross section of $13.8_{-3.8}^{+4.3}(\text{stat})_{-0.9}^{+1.2}(\text{syst}) \pm 0.9(\text{lum})$ pb, in agreement with predictions from the standard model.

PACS numbers: 13.38.Be, 14.70.Fm

The measurement of the W boson pair-production cross section $\sigma_{p\bar{p} \rightarrow W^+W^-}$ offers a good opportunity to test the non-Abelian structure of the standard model (SM). Furthermore, this measurement is sensitive to new phenomena since anomalous trilinear couplings [1] or

the production and decay of new particles such as the Higgs boson [2] would enhance the rate of W boson pair-production. The next-to-leading order (NLO) calculations for $\sigma_{p\bar{p} \rightarrow W^+W^-}$ [3] predict a cross section of 12.0–13.5 pb at $\sqrt{s} = 1.96$ TeV. The CDF Collaboration

reported evidence for W boson pair-production, based on 108 pb^{-1} of data collected in Run I of the Fermilab Tevatron Collider at $\sqrt{s} = 1.8 \text{ TeV}$, with a cross section $\sigma_{p\bar{p} \rightarrow W^+W^-} = 10.2_{-5.1}^{+6.3}(\text{stat}) \pm 1.6(\text{syst}) \text{ pb}$ [4].

In this Letter we present a measurement of the W^+W^- production cross section in leptonic final states $p\bar{p} \rightarrow W^+W^- \rightarrow \ell^+\nu\ell^-\bar{\nu}$ ($\ell = e, \mu$). We use data collected between April 2002 and March 2004 in $p\bar{p}$ collisions at $\sqrt{s} = 1.96 \text{ TeV}$ of Run II of the Tevatron Collider. The integrated luminosities are $252 \pm 16 \text{ pb}^{-1}$, $235 \pm 15 \text{ pb}^{-1}$, and $224 \pm 15 \text{ pb}^{-1}$ for the e^+e^- , $e^\pm\mu^\mp$, and $\mu^+\mu^-$ channels, respectively. The differences in the integrated luminosities for various channels are primarily due to different trigger conditions.

We briefly describe the main components of the DØ Run II detector [5] important to this analysis. The central tracking system consists of a silicon microstrip tracker (SMT) and a central fiber tracker (CFT), both located within a 2.0 T axial magnetic field. The SMT strips have a typical pitch of 50–80 μm , and the design is optimized for tracking and vertexing over the pseudorapidity range $|\eta| < 3$, where $\eta = -\ln(\tan\frac{\theta}{2})$ with polar angle θ . The system has a six-barrel longitudinal structure, each with a set of four silicon layers arranged axially around the beam pipe, interspersed with sixteen radial disks. The CFT has eight thin coaxial barrels, each supporting two doublets of overlapping scintillating fibers of 0.835 mm diameter, one doublet parallel to the beam axis, the other alternating by $\pm 3^\circ$ relative to the beam axis.

A liquid-argon/uranium calorimeter surrounds the central tracking system and consists of a central calorimeter (CC) covering to $|\eta| \approx 1.1$, and two end calorimeters (EC) extending coverage for $|\eta| < 4.2$, all housed in separate cryostats [6]. Scintillators between the CC and EC cryostats provide sampling of showers for $1.1 < |\eta| < 1.4$.

The muon system is located outside the calorimeters and consists of a layer of tracking detectors and scintillation trigger counters inside toroid magnets which provide a 1.8 T magnetic field, followed by two similar layers behind each toroid. Tracking in the muon system for $|\eta| < 1$ relies on 10 cm wide drift tubes [6], while 1 cm mini-drift tubes are used for $1 < |\eta| < 2$ [7].

The $W^+W^- \rightarrow \ell^+\nu\ell^-\bar{\nu}$ candidates are selected by triggering on single or di-lepton events using a three level trigger system. The first trigger level uses hardware to select electron candidates based on energy deposition in the electromagnetic part of the calorimeter and selects muon candidates formed by hits in two layers of the muon scintillator system. Digital signal processors in the second trigger level form muon track candidate segments defined by hits in the muon drift chambers and scintillators. At the third level, software algorithms running on a computing farm and exploiting the full event information are used to make the final selection of events which are recorded for offline analysis.

In the further offline analysis electrons are identified by electromagnetic showers in the calorimeter. These showers are chosen by comparing the longitudinal and transverse shower profiles to those of simulated electrons. The showers must be isolated, deposit most of their energy in the electromagnetic part of the calorimeter, and pass a likelihood criterion that includes a spatial track match and, in the CC region, an E/p requirement, where E is the energy of the calorimeter cluster and p is the momentum of the track. All electrons are required to be in the pseudorapidity range $|\eta| < 3.0$. The transverse momentum measurement of the electrons is based on calorimeter cell energy information.

Muon tracks are reconstructed from hits in the wire chambers and scintillators in the muon system and must match a track in the central tracker. To select isolated muons, the scalar sum of the transverse momentum of all tracks other than that of the muon in a cone of $\mathcal{R} = 0.5$ around the muon track must be less than 4 GeV, where $\mathcal{R} = \sqrt{(\Delta\phi)^2 + (\Delta\eta)^2}$ and ϕ is the azimuthal angle. Muon detection is restricted to the coverage of the muon system $|\eta| < 2.0$. Muons from cosmic rays are rejected by requiring a timing criterion on the hits in the scintillator layers as well as applying restrictions on the position of the muon track with respect to the primary vertex.

The decay of two W bosons into electrons or muons results in three different final states $e^+e^- + X$ (ee channel), $e^\pm\mu^\mp + X$ ($e\mu$ channel), and $\mu^+\mu^- + X$ ($\mu\mu$ channel), each of which consists of two oppositely charged isolated high transverse momentum, p_T , leptons and large missing transverse energy, \cancel{E}_T , due to the escaping neutrinos. The selection criteria for each channel were chosen to maximize the the expected signal significance, while keeping high efficiency for WW production.

In all three channels, two leptons originating from the same vertex are required to be of opposite charge, and must have $p_T > 20 \text{ GeV}$ for the leading lepton and $p_T > 15 \text{ GeV}$ for the trailing one. Figure 1 shows the good agreement between data and Monte Carlo (MC) in \cancel{E}_T distributions for the ee channel (a), the $\mu\mu$ channel (c) and the $e\mu$ channel (e) after applying the lepton transverse momentum cuts. In all cases, the background is largely dominated by Z/γ^* production which is suppressed by requiring the \cancel{E}_T to be greater than 30 GeV, 40 GeV, and 20 GeV in the ee , $\mu\mu$, and $e\mu$ channels, respectively. The different cut values among the three channels are due to the different momentum resolution of electrons and muons.

In the ee channel, additional cuts are applied to further reduce the Z/γ^* background and other backgrounds. The minimal transverse mass $m_T^{\text{min}} = \min(m_T^{e_1}, m_T^{e_2})$ must exceed 60 GeV, where $m_T = \sqrt{2\cancel{E}_T p_T^e (1 - \cos\Delta\phi(p_T^e, \cancel{E}_T))}$. Events are removed if the invariant di-electron mass is between 76 and 106 GeV. Events are also removed if the \cancel{E}_T has a large contribution from the mismeasurement of jet energy, using the follow-

ing procedure. The fluctuation in the measurement of jet energy in the transverse plane can be approximated by $\Delta E_T^{\text{jet}} \cdot \sin \theta^{\text{jet}}$ where ΔE_T^{jet} is proportional to $\sqrt{E_T^{\text{jet}}}$. The opening angle $\Delta\phi(\text{jet}, \cancel{E}_T)$ between this projected energy fluctuation and the missing transverse energy provides a measure of the contribution of the jet to the missing transverse energy. The scaled missing transverse energy defined as

$$\cancel{E}_T^{\text{Sc}} = \frac{\cancel{E}_T}{\sqrt{\sum_{\text{jets}} (\Delta E_T^{\text{jet}} \cdot \sin \theta^{\text{jet}} \cdot \cos \Delta\phi(\text{jet}, \cancel{E}_T))^2}} \quad (1)$$

is required to be greater than 15. Finally, to suppress the background from $t\bar{t}$ production, the scalar sum of the transverse energies of all jets with $E_T^{\text{jet}} > 20$ GeV and $|\eta| < 2.5$, H_T , is required to be less than 50 GeV. Figure 1(b) shows the \cancel{E}_T distribution after the final selection without applying the \cancel{E}_T criterion for the ee channel, and Fig. 2(a) shows the distribution of the minimal transverse mass after applying all selection criteria except the cut on the minimal transverse mass. Six events remain in the ee data sample after all of these cuts are applied.

For the $\mu\mu$ channel, to further reduce the Z/γ^* background, only events with an invariant di-muon mass between 20 and 80 GeV are retained. Since the momentum resolution is worsening for high p_T tracks, an additional constrained fit is performed to reject events compatible with Z boson production. The opening angle between the two muons in the transverse plane is required to be $\Delta\phi_{\mu\mu} < 2.4$. Finally, requiring $H_T < 100$ GeV removes the remaining background from $t\bar{t}$ events. Figure 1(d) shows the \cancel{E}_T distribution after the final selection without applying the \cancel{E}_T criterion for the $\mu\mu$ channel. Four events are observed in the $\mu\mu$ data sample after application of all selection criteria.

In the $e\mu$ channel, to suppress the WZ and ZZ background, events are rejected if a third lepton is found and the invariant mass of two leptons of the same flavor and opposite charge is in the range from 61 to 121 GeV. To remove background from multijet production and $Z/\gamma^* \rightarrow \tau\tau$ events, the minimal transverse mass $m_T^{\text{min}} = \min(m_T^e, m_T^\mu)$ must exceed 20 GeV. The remaining $Z/\gamma^* \rightarrow \tau\tau$ events are suppressed by removing events with $\cancel{E}_T^{\text{Sc}} < 15$. Requiring $H_T < 50$ GeV rejects most of the $t\bar{t}$ events. To remove $W + \gamma$ events in which photons convert to electron-positron pairs, at least three hits in the silicon tracker are required for the electron track if the transverse mass determined from the muon and \cancel{E}_T is consistent with the W boson transverse mass. Figure 1(f) shows the \cancel{E}_T distribution after the final selection without applying the \cancel{E}_T criterion for the $e\mu$ channel, whereas Fig. 2(b) shows the distribution of the minimal transverse mass after applying all selection criteria except the cut on the minimal transverse mass. Fifteen events survive the final selection criteria in the $e\mu$ data sample.

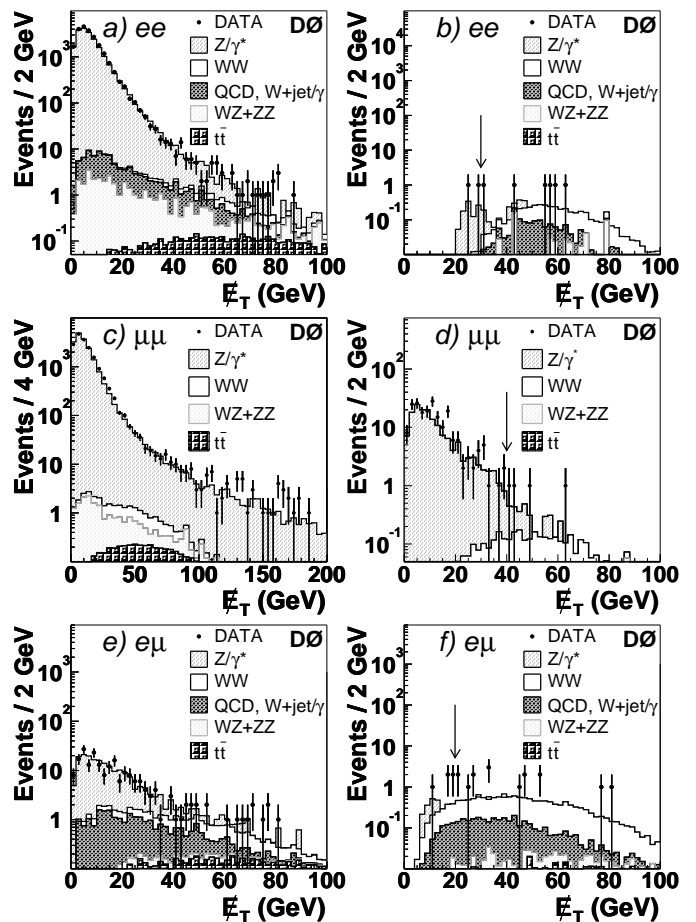


FIG. 1: Distribution of the missing transverse energy \cancel{E}_T after applying the initial transverse momentum cuts in the (a) ee , (c) $\mu\mu$, and (e) $e\mu$ channel. Figures (b), (d), and (f) show the \cancel{E}_T distributions after the final selection except for the \cancel{E}_T criterion for the ee , $\mu\mu$, and $e\mu$ channel, respectively. The arrows indicate the cut values. QCD contribution is negligible in Figs. (c) and (d).

The efficiency for WW signal events to pass the acceptance and kinematic criteria is determined using the PYTHIA 6.2 [8] event generator followed by a detailed GEANT-based [9] simulation of the $D0$ detector. All trigger and reconstruction efficiencies are derived from the data. For the ee channel, the overall detection efficiency is $(8.76 \pm 0.13)\%$. The overall efficiencies for the $\mu\mu$ and $e\mu$ channels are $(6.22 \pm 0.15)\%$ and $(15.40 \pm 0.20)\%$, respectively. Using an NLO cross section of 13.5 pb [3] and branching fractions B of 0.1072 ± 0.0016 for $W \rightarrow e\nu$ and 0.1057 ± 0.0022 for $W \rightarrow \mu\nu$ [10], the expected number of events for the pair production of W bosons combined for all three channels is $16.6 \pm 0.1(\text{stat}) \pm 0.6(\text{syst}) \pm 1.1(\text{lum})$ events, where the statistical error is given by the statistics of the MC sample. The signal breakdown for the three channels is given by the first line of Table I.

Background contributions from Z/γ^* , $W+\text{jet}/\gamma$, $t\bar{t}$, WZ and ZZ events are estimated using the PYTHIA event

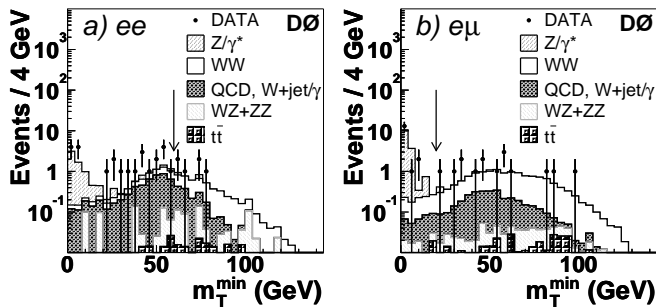


FIG. 2: Distribution of the minimal transverse mass m_T^{\min} after applying all selection criteria except the cut on m_T^{\min} for the (a) ee and the (b) $e\mu$ channel. The arrows indicate the cut values.

generator. In addition, W +jet/ γ contributions are verified using ALPGEN [11]. All events are processed through the full detector simulation. The background due to multijet production, when a jet is misidentified as an electron, is determined from the data using a sample of like-sign di-lepton events with inverted lepton quality cuts (called QCD background in Figs. 1 and 2).

For the normalization of Z/γ^* and W +jet/ γ events, the NNLO cross sections from Ref. [12] are used. The cross section times branching ratio of Z/γ^* production in the invariant mass region $60 \text{ GeV} < m_{\ell\ell} < 130 \text{ GeV}$ is $\sigma \times B = 254 \text{ pb}$. For inclusive W boson production with decays into a single lepton flavor state, this value is $\sigma \times B = 2717 \text{ pb}$. The NLO WZ and ZZ production cross section values are taken from Ref. [3] with $\sigma \times B = 0.014 \text{ pb}$ for WZ and $\sigma \times B = 0.002 \text{ pb}$ for ZZ production with decay into a single lepton flavor state. The calculations of Ref. [13] are used for $t\bar{t}$ production with $\sigma \times B = 0.076 \text{ pb}$ with single flavor lepton decays of both W bosons. A summary of the background contributions together with signal expectations and events observed in the data after the final selection for the individual channels is shown in Table I. The total background sum is $8.1 \pm 0.6(\text{stat}) \pm 0.6(\text{syst}) \pm 0.5(\text{lum})$ events. The $e\mu$ channel has both the highest signal efficiency and best signal-to-background ratio. There is good agreement between the number of events observed in the data and the sum of the expectations from WW production and the various backgrounds in all three channels.

Systematic uncertainties that affect the WW production cross section measurement are listed in Table II. In these estimates, parameters are varied within $\pm 1\sigma$ of the respective theoretical or experimental errors. Sources such as the trigger efficiency, electron and muon identification (ID) efficiencies, jet energy scale (JES), electron and muon momentum resolution, branching fraction $B(W \rightarrow \ell\nu)$, cross section calculation of Z/γ^* and $t\bar{t}$ events, and the determination of W +jet/ γ background contribute to the systematic uncertainty. The PYTHIA Monte Carlo tends to underestimate jet multiplicities,

TABLE I: Number of signal and background events expected and number of events observed after all selections are applied for the three channels. Only statistical uncertainties are given.

Process	ee	$e\mu$	$\mu\mu$
WW signal	3.42 ± 0.05	11.10 ± 0.10	2.10 ± 0.05
$Z/\gamma^* \rightarrow ee$	0.20 ± 0.06	—	—
$Z/\gamma^* \rightarrow \mu\mu$	—	0.28 ± 0.09	1.60 ± 0.40
$Z/\gamma^* \rightarrow \tau\tau$	< 0.01	0.0 ± 0.1	< 0.01
$t\bar{t}$	0.18 ± 0.02	0.34 ± 0.03	0.09 ± 0.01
WZ	0.33 ± 0.17	0.38 ± 0.02	0.15 ± 0.08
ZZ	0.19 ± 0.06	0.02 ± 0.02	0.10 ± 0.04
W +jet/ γ	1.40 ± 0.07	2.72 ± 0.07	0.01 ± 0.01
Multijet	< 0.05	0.07 ± 0.07	< 0.05
Background sum	2.30 ± 0.21	3.81 ± 0.17	1.95 ± 0.41
Data	6	15	4

TABLE II: Systematic uncertainties for the ee , $e\mu$, and $\mu\mu$ channels.

Source	Change in the WW cross section (%)					
	ee		$e\mu$		$\mu\mu$	
Trigger, ID	+4.7	-4.6	+3.9	-3.8	+6.2	-5.8
JES	+3.2	-3.2	+1.6	-1.2	+7.2	-4.8
μ resolution	—	—	+4.7	-2.2	+10.0	-4.1
e resolution	+4.6	-2.9	+1.3	-1.1	—	—
$B(W \rightarrow \ell\nu)$	+4.4	-3.9	+5.3	-4.6	+4.3	-4.1
$\sigma(Z/\gamma^*, t\bar{t})$	+0.9	-0.7	+0.4	-0.4	+3.2	-3.2
W +jet/ γ	+4.0	-4.0	+3.0	-3.0	—	—
Re-weighting	+4.3	-4.4	—	—	+1.5	-1.5
Total	+10.3	-9.5	+8.9	-7.3	+14.9	-10.1

since a parton-shower approach is used for initial and final state radiation instead of the full matrix element. To compensate for this underestimation, events are re-weighted in the MC to reproduce the jet multiplicities seen in the data. The systematic uncertainty for this approach is determined from a measurement of the WW production cross section with and without the re-weighting. The total systematic uncertainties are given in Table II. The uncertainty on the luminosity measurement is 6.5%.

The cross section for W boson pair production is estimated using a likelihood method [14, 15] with Poisson statistics. The cross section for each channel $\sigma_{p\bar{p} \rightarrow W^+W^-}$ is given by

$$\sigma_{p\bar{p} \rightarrow W^+W^-} = \frac{N_{\text{obs}} - N_{bg}}{\int \mathcal{L} dt \cdot B \cdot \epsilon}, \quad (2)$$

where N_{obs} is the number of observed events, N_{bg} is the expected background, $\int \mathcal{L} dt$ is the integrated luminosity, B is the branching fraction for $W \rightarrow \ell\nu$, and ϵ is the efficiency for the signal. The likelihood for N_{obs} events

in the data is given by

$$L(\sigma_{p\bar{p}\rightarrow W^+W^-}, N_{\text{obs}}, N_{bg}, \int \mathcal{L}dt, B, \epsilon) = \frac{N^{N_{\text{obs}}}}{N_{\text{obs}}!} e^{-N}, \quad (3)$$

where N is the number of signal and background events:

$$N = \sigma_{p\bar{p}\rightarrow W^+W^-} \cdot B \cdot \int \mathcal{L}dt \cdot \epsilon + N_{bg}. \quad (4)$$

The cross section $\sigma_{p\bar{p}\rightarrow W^+W^-}$ is estimated by minimizing $-2 \ln L(\sigma_{p\bar{p}\rightarrow W^+W^-}, N_{\text{obs}}, N_{bg}, \int \mathcal{L}dt, B, \epsilon)$. To combine the channels, the individual likelihood functions are multiplied. As a final result, the combined cross section for WW production at a center-of-mass energy of $\sqrt{s} = 1.96$ TeV is

$$\sigma_{p\bar{p}\rightarrow W^+W^-} = 13.8_{-3.8}^{+4.3}(\text{stat}) \quad {}_{-0.9}^{+1.2}(\text{syst}) \pm 0.9(\text{lum}) \text{ pb}. \quad (5)$$

This value is in good agreement with the NLO calculation prediction of 12.0–13.5 pb at $\sqrt{s} = 1.96$ TeV [3].

The significance for the signal observation can be estimated using the likelihood ratio method [16]. The confidence levels for a background only hypothesis, CL_B , is obtained using the background expectation and the number of events observed as input. The signal significance is extracted from $1 - CL_B$. The probability of an upward fluctuation of the background is 2.3×10^{-7} , which corresponds to 5.2 standard deviations for a Gaussian probability distribution.

To conclude, we have measured the W boson pair production cross section in $p\bar{p}$ collisions at $\sqrt{s} = 1.96$ TeV. We observe 25 events in the data, corresponding to integrated luminosities of 224–252 pb $^{-1}$ depending on the final state, with a background expectation from non- WW processes of $8.1 \pm 0.6(\text{stat}) \pm 0.6(\text{syst}) \pm 0.5(\text{lum})$ events. The expectation for SM pair production of W bosons in our data sample is $16.6 \pm 0.1(\text{stat}) \pm 0.6(\text{syst}) \pm 1.1(\text{lum})$ events. We obtain a production cross section of $\sigma_{p\bar{p}\rightarrow W^+W^-} = 13.8_{-3.8}^{+4.3}(\text{stat}) \quad {}_{-0.9}^{+1.2}(\text{syst}) \pm 0.9(\text{lum})$ pb, consistent with the NLO prediction. The probability that the observed events are caused by a fluctuation of the background is 2.3×10^{-7} , corresponding to 5.2 standard deviations.

We thank the staffs at Fermilab and collaborating institutions, and acknowledge support from the Department of Energy and National Science Foundation (USA), Commissariat à l'Énergie Atomique and CNRS/Institut National de Physique Nucléaire et de Physique des Particules (France), Ministry of Education and Science, Agency for Atomic Energy and RF President Grants Program (Russia), CAPES, CNPq, FAPERJ, FAPESP and FUNDUNESP (Brazil), Departments of Atomic Energy

and Science and Technology (India), Colciencias (Colombia), CONACyT (Mexico), KRF (Korea), CONICET and UBACyT (Argentina), The Foundation for Fundamental Research on Matter (The Netherlands), PPARC (United Kingdom), Ministry of Education (Czech Republic), Natural Sciences and Engineering Research Council and WestGrid Project (Canada), BMBF and DFG (Germany), A.P. Sloan Foundation, Research Corporation, Texas Advanced Research Program, and the Alexander von Humboldt Foundation.

-
- [*] Visitor from University of Zurich, Zurich, Switzerland.
[†] Visitor from Institute of Nuclear Physics, Krakow, Poland.
- [1] DØ Collaboration, B. Abbott *et al.*, Phys. Rev. D **60**, 072002 (1999); K. Hagiwara, J. Woodside, and D. Zeppenfeld, Phys. Rev. D **41**, 2113 (1990).
[2] E. Eichten, I. Hinchliffe, K. Lane, and C. Quigg, Rev. Mod. Phys. **56**, 579 (1984); Addendum *ibid.* **58**, 1065 (1986).
[3] J. Ohnemus, Phys. Rev. D **44**, 1403 (1991); J. Ohnemus, Phys. Rev. D **50**, 1931 (1994); J. M. Campbell and R. K. Ellis, Phys. Rev. D **60**, 113006 (1999).
[4] CDF Collaboration, F. Abe *et al.*, Phys. Rev. Lett. **78**, 4536 (1997).
[5] DØ Collaboration, V. Abazov *et al.*, to be submitted to Nucl. Instrum. Methods A; T. LeCompte and H.T. Diehl, Ann. Rev. Nucl. Part. Sci. **50**, 71 (2000).
[6] DØ Collaboration, S. Abachi *et al.*, Nucl. Instrum. Methods Phys. Res. A **338**, 185 (1994).
[7] V. Abramov *et al.*, Nucl. Instrum. Meth. A **419**, 660 (1998).
[8] T. Sjöstrand *et al.*, Comp. Phys. Comm. **135**, 238 (2001).
[9] R. Brun and F. Carminati, CERN Program Library Long Writeup W5013, 1993 (unpublished).
[10] Particle Data Group, S. Eidelman *et al.*, Phys. Lett. B **592**, 1 (2004).
[11] M.L. Mangano *et al.*, J. High Energy Phys. **0307**, 001 (2003).
[12] R. Hamberg, W.L. van Neerven, and T. Matsuura, Nucl. Phys. **B359**, 343 (1991) [Erratum-*ibid.* **B644**, 403 (2002)].
[13] N. Kidonakis and R. Vogt, Phys. Rev. D **68**, 114014 (2003).
[14] G. J. Feldman and R. D. Cousins, Phys. Rev. D **57**, 3873 (1998).
[15] B. P. Roe and M. B. Woodroffe, Phys. Rev. D **60**, 053009 (1999).
[16] T. Junk, Nucl. Instrum. Methods A **434**, 435 (1999).